Antioxidant Nitrone Scaffold Based on Plant Pigments

Amanda Capistrano Pinheiro[†], Rodrigo Boni Fazzi[†], Larissa Cerrato Esteves[†], Caroline Oliveira Machado[†], Felipe Augusto Dörr[‡], Ernani Pinto[‡], Yocefu Hattori[§], Jacinto Sa[§,∥], Ana Maria da Costa Ferreira[†], and Erick Leite Bastos[†,*]

[†] Departamento de Química Fundamental, Instituto de Química, Universidade de São Paulo, 05508-000 São Paulo, SP, Brazil

[‡] Departamento de Análises Clínicas e Toxicológicas, Faculdade de Ciências Farmacêuticas, Universidade de São Paulo, 05508-000 São Paulo, SP, Brazil

[§] Physical Chemistry Division, Department of Chemistry, Ångström Laboratory, Uppsala University, 75120 Uppsala, Sweden

[∥] Institute of Physical Chemistry, Polish Academy of Sciences, 01-224 Warsaw, Poland

[*] Corresponding author: elbastos@iq.usp.br

ABSTRACT

Nitrones derived from natural antioxidants are emerging as highly specific therapeutics against various human diseases, including stroke, neurodegenerative pathologies, and cancer. However,

the development of useful pseudo-natural nitrones requires the judicious choice of a secondary metabolite as the precursor. Betalains are nitrogen-containing natural pigments that exhibit marked antioxidant capacity and pharmacological properties and, hence, are ideal candidates for designing multifunctional nitrones. In this work, we describe the semisynthesis and properties of a biocompatible, antioxidant betalain-nitrone called OxiBeet. This bio-based compound is a better radical scavenger than ascorbic acid, gallic acid, and most non-phenolic antioxidants and undergoes concerted proton-coupled electron transfer. The autoxidation of OxiBeet produces a persistent nitroxide radical, which, herein, is studied via electron paramagnetic resonance spectroscopy. In addition, femtosecond transient absorption spectroscopy reveals that excited state formation is not required for the oxidation of OxiBeet. The results are compared with those obtained using betanin, a natural betalain, and pBeet, the imine analog of OxiBeet. The findings of this study will enable the development of antioxidant nitrones based on the novel *N*-oxide 1,7-diazaheptamethinium scaffold and betalain dyes with enhanced hydrolytic stability in aqueous alkaline media.

INTRODUCTION

The formation of stable and persistent nitroxide adducts of free radical reactive species endows nitrones with marked antioxidant potential and supports their use as therapeutic agents to treat disorders related to oxidative stress.[1-3] The same process promotes the use of nitrones as building blocks for the construction of nitrogenous compounds[4] and as electron paramagnetic resonance (EPR) spin traps.[5] Although natural products containing the nitrone functional group are scarce,[6] antioxidant and pharmacologically active compounds of natural origin can be used as starting materials for the semisynthesis of novel nitrones that have many potential applications.

Antioxidants based on natural product scaffolds help reduce the demand for non-renewable hydrocarbon resources and are highly valued in medicinal chemistry and drug discovery.[7, 8] The nitrone derivatives of ligustrazine— a pyrazine found in the Chinese herb *Ligusticum wallichii* Franch.—have antioxidant and thrombolytic properties and are effective therapeutics for treating ischemic stroke.[3] Another important example is the nitrone derived from the water-soluble analog of vitamin E (Trolox), which shows enhanced radical scavenging and neuroprotective properties.[9]

Betalains are non-toxic water-soluble pigments found in plants, fungi, and bacteria[10] that have been consumed for millennia.[10-12] Indeed, betanin (5-*O*-β-glucosyl betanidin, EFSA/E162 and FDA/73.40) and indicaxanthin (L-proline-betaxanthin), the main pigments in red beetroots (*Beta vulgaris* L.) and prickly pears [*Opuntia ficus indica* (L.) Mill.], respectively, positively affect the in vivo redox states.[13-17] Both phenolic and non-phenolic betalains are highly efficient dietary antioxidants,[14] outperforming vitamin C, vitamin E, and many flavonoids in terms of antioxidant capacity (i.e., thermodynamics, the number of radicals scavenged) and activity (i.e., kinetics, reactivity towards radicals).[14, 18-20]

Here, we describe the semisynthesis and properties of OxiBeet— the first betalain-nitrone to be reported in the literature. This bioinspired molecule is stable towards hydrolysis under neutral and slightly alkaline conditions, and it is not cytotoxic to the human hepatic cell line HepaRG at concentrations of up to 1 mM. OxiBeet has a high radical scavenging capacity and low reduction potential. Furthermore, it can be converted into a persistent *N*-oxide 1,7-diazaheptamethinium radical cation via autoxidation in an aqueous solution. A comparison of the characteristics of OxiBeet with those of natural betalains and pBeet provides new insights into the use of polymethine dyes to develop resonance-stabilized radicals.

MATERIALS AND METHODS

General information

All chemicals were purchased from Sigma-Aldrich and used without further purification unless otherwise stated. Betalamic acid was extracted from base-hydrolyzed red beetroot juice and processed as described previously.[21, 22] Aqueous solutions were prepared using deionized water (18.2 MΩ cm at 25 °C, TOC ≤ 4 ppb, Milli-Q, Millipore). Additional experimental details are available in the Supporting Information.

Semisynthesis of OxiBeet

N-Phenylhydroxylamine (13.5 mg, 125 μmol, 5.0 equiv) was added to an aqueous solution of betalamic acid (5.3 mg, 25 μmol, 1.0 equiv) that had been acidified with HCl (25 mL, pH 3). The mixture was maintained at 4 ± 1 °C for 1 h; the resulting red–orange solution was subjected to flash gel permeation chromatography (Sephadex LH-20, water, 1.5 × 20 cm, 20 psi). The orange-colored fraction was lyophilized (–80 °C, 0.08 mbar) to obtain OxiBeet (phenylhydroxylamine-betaxanthin, 3.8 mg, 50%) as an orange solid.

¹H-NMR (800 MHz, D₂O): δ 8.32 (d, J = 10.4 Hz, 1H), 7.60 (d, J = 7.9 Hz, 2H), 7.52 (t, J = 7.9 Hz, 2H), 7.46-7.41 (m, 1H), 7.09 (d, J = 10.4 Hz, 1H), 6.50 (bs, 1H), 4.27 (bs, 1H), 3.22 (bs, 1H), 3.10 (dd, J = 17.1, 7.5 Hz, 1H).

¹³C-NMR (200 MHz, D₂O): δ 179.84, 170.39, 160.41, 153.81, 146.46, 132.24, 131.53, 122.67, 118.30, 109.77, 57.02, 30.51.

HRMS (ESI(+)-TOF): Calc'd for $C_{15}H_{15}N_2O_5^+$, [M]⁺, 303.0975; found 303.0976; diff. 0.3 ppm.

UV–Vis: λ_{abs}^{max} = 460 nm, $\varepsilon^{460\,nm}$ = 35,000 ± 2400 L mol^{-1} cm^{-1} (pH 6) (Figs. S1 and S2).

Fluorescence (Fl): λ_{Fl}^{max} = 562 nm (pH 6, λ^{EX} = 460 nm).

MTT assay

HepaRG cells were cultured until confluence in Dulbecco's Modified Eagle Medium (DMEM) supplemented with 10% (v/v) fetal bovine serum (FBS). Cells were seeded in a 96-well plate (5×10^3 cells/well) and treated with OxiBeet in 1% FBS DMEM (mmol L^{-1} to μmol L^{-1}) for 6 h at 37 °C. Negative and positive control experiments were conducted using 1% FBS DMEM and Triton X-100 1% (v/v) in phosphate-buffered saline (PBS), respectively. A solution of MTT (3-[4,5-dimethylthiazol-2-yl]-2,5-diphenyltetrazolium bromide) in 1% FBS DMEM (5 mg mL^{-1}, 10% (v/v)) was added to each well. After incubating for 30 min at 37 °C, the medium was removed and replaced with DMSO (100 μL). The absorption of the resulting purple formazan solution was measured at 550 nm, and cell viability was calculated as the absorbance percentage of the sample relative to that of the negative control.

Radical scavenging capacity

Radical scavenging capacity was determined using the TEAC/ABTS$^{+\bullet}$ assay.[23] A solution of ABTS$^{+\bullet}$/ABTS in phosphate buffer (50 mmol L^{-1}, pH 7.4) with an absorbance of 0.7 at 734 nm (46.7 μmol L^{-1} ABTS$^{+\bullet}$) was prepared. The bleaching of ABTS$^{+\bullet}$ by the antioxidant (μmol L^{-1} concentration range) was monitored at 734 nm for 6 min at 25 °C. The slope α of the linear correlation between the change in absorption ΔAbs and the antioxidant concentration was measured. The Trolox equivalent antioxidant capacity (TEAC) was calculated as the ratio between the value of α for the sample and that of the Trolox standard, $\alpha_{Sample}/\alpha_{Trolox}$.

Cyclic voltammetry

Cyclic voltammetry was conducted at 25 °C using a Metrohm Autolab PGSTAT101 potentiostat/galvanostat equipped with a 10-mL electrochemical cell and controlled using the proprietary NOVA software. A glassy carbon working electrode (diameter of electrode disk = 2 mm), a platinum wire auxiliary electrode, and an Ag/AgCl (KCl sat.) reference electrode were used; the potential range was –0.2 to 0.8 V, the scan rate was 50 mV s^{-1}, and the analyte concentration was 88 µmol L^{-1} in aqueous KCl (0.1 mol L^{-1}) at pH 7.0. Before each experiment, the working electrode was polished with 0.05-µm alumina particles (60 cycles) and sonicated with water for 1 min.

EPR spectroscopy and simulation

X-band EPR spectra were obtained at room temperature (20 ± 2 °C) using a Bruker EMX spectrometer equipped with a standard cavity and operated at approximately 9.7 GHz with a 100 kHz modulation frequency (spectrometer settings: 20 mW microwave power, 0.5 G modulation amplitude, 20.48 ms time constant, 1024 points, 100 G scan range). The 2,2-diphenyl-1-picrylhydrazyl (DPPH) radical (g-value = 2.0036) was used to calibrate the magnetic field. pBeet and OxiBeet solutions (1 mmol L^{-1}) were prepared immediately before use in aerated phosphate buffer (50 mmol L^{-1}, pH 7.4) and maintained at room temperature. All analyses were conducted using 200 µL of the respective solution in a suprasil flat cell (Wilmad). EPR simulations were carried out using the Easyspin toolbox in MATLAB.[24] The simulation was fitted to the experimental spectra using the Nelder–Mead simplex method. The following parameters were used: g-value = 2.0059; a_α^N = 33.6 MHz, a_β^H = 17.6 MHz, a_γ^H = 9.2 MHz and $a_\gamma^{2\times H}$ = 8.2 MHz;

line width for isotropic broadening and full width at half maximum (FWHM) = 0.01% Gaussian and 0.29% Lorentzian.

Transient absorption spectroscopy

Femtosecond pump-probe transient absorption measurements were performed using a regenerative amplified Ti:sapphire laser system (Coherent Libra Ultrafast Amplifier System; 795 nm, FWHM $\approx$ 40 fs, 1 mJ/pulse, 3 kHz repetition rate) as the laser source and a Newport MS260i imaging spectrograph. Briefly, the 795 nm output pulse from the regenerative amplifier was split into two by a 50:50 beam splitter. The transmitted part was directed into an optical parametric amplifier (TOPAS-prime, Light Conversion) to generate a pump beam at 485 nm (1 mW ± 2%), which was focused on the sample with a beam diameter of ca. 300 μm. The reflected beam was passed through a delay stage (8.5 ns; 1–2 fs step size) and focused on a sapphire crystal to generate a white light continuum, which was used as the probe beam. The pump pulses were chopped by a synchronized chopper at 1500 Hz, and the absorbance change was calculated by using the spectroscopic measurements obtained from two adjacent probe pulses, one acquired with the pump beam blocked and the second with the pump beam unblocked. The samples were placed in 1-mm quartz cuvettes and the spectra of all the samples were acquired under ambient conditions.
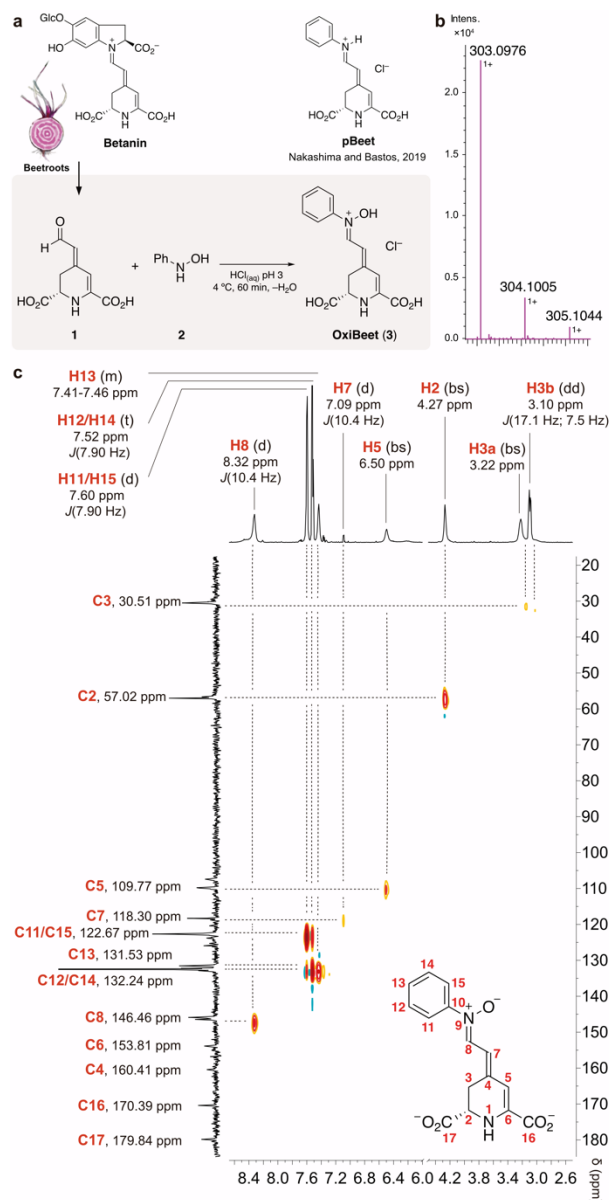
RESULTS AND DISCUSSION

OxiBeet was semisynthesized as shown in Fig. 1a. Betalamic acid (**1**) was produced by the hydrolysis of the betalains in red beetroot juice, but it can also be obtained by enzymatic oxidation of L-DOPA[25]. The coupling between **1** and *N*-phenylhydroxylamine (**2**) in acidified water is quantitative and gives rise to OxiBeet (**3**). The product was isolated in 50% yield after

purification in the presence of oxygen, which is twice as high as the values reported for other betalains.[20, 26] The high-resolution mass spectrum was consistent with the postulated structure of OxiBeet (Fig. 1b). Notably, both the semisynthesis and purification of **3** involved water as solvent, and **2** can be produced using environmentally benign methods.[27]

The high persistence and solubility of OxiBeet in water enable its characterization using nuclear magnetic resonance (NMR) spectroscopy (Fig. 1c), which is rarely used to study betalains because of their lability and low solubility in organic media.[28, 29] The coupling constant between the H7 and H8 atoms of OxiBeet ($^3J_{H7,H8}$ = 10.4 Hz) is slightly smaller than the values typically reported for natural betalains ($^3J_{H7,H8} \sim$ 12 Hz).[30] The H7 and C5 atoms of OxiBeet are more deshielded (by ca. 1 ppm and 10 ppm, respectively) compared to those of betanin and indicaxanthin.[28, 30] Hence, the mesomeric donation of electron density by the oxygen atom of the nitrone group into the π-system decreases the electrophilicity of the C8 and improves the hydrolytic stability of OxiBeet compared to natural analogs.
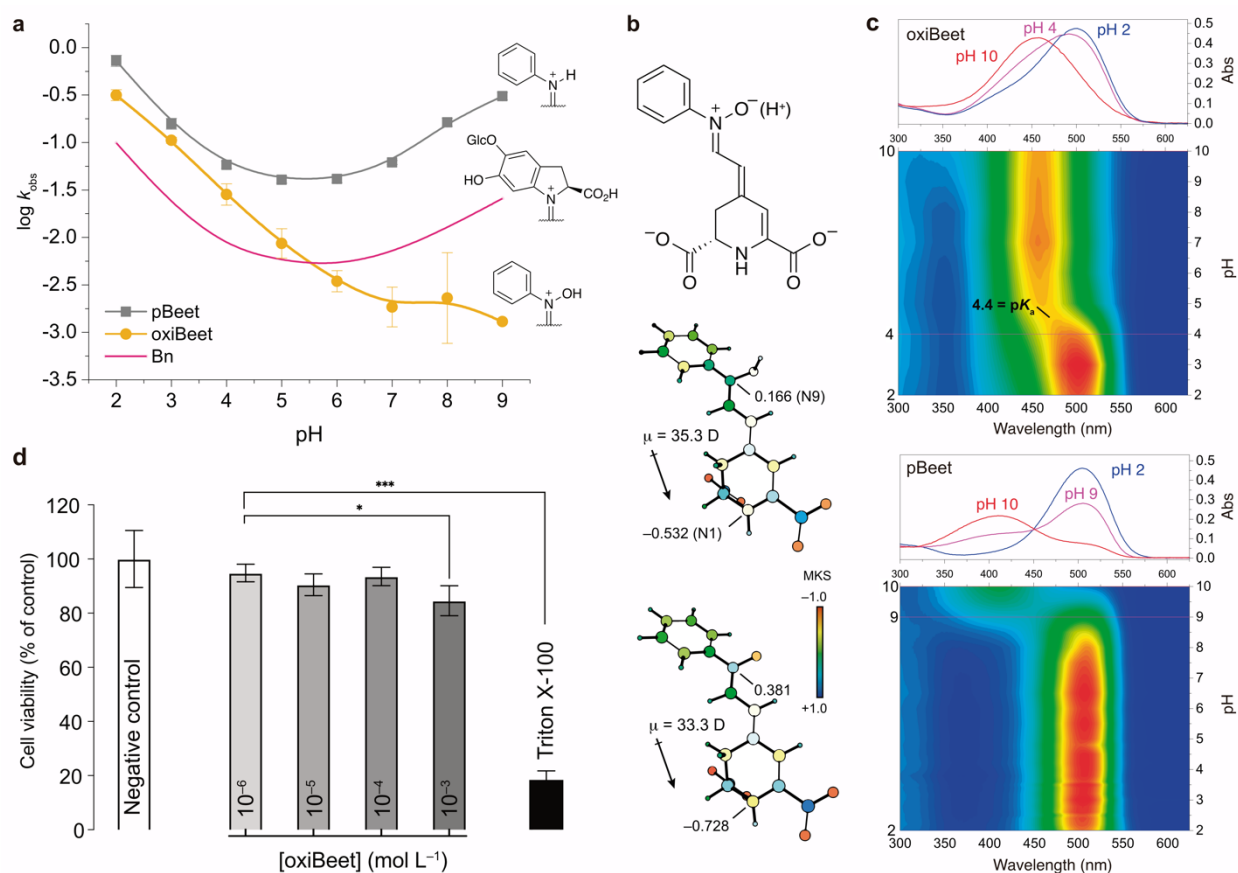
Figure 1. Semisynthesis and characterization of OxiBeet. (a) Acid-catalyzed coupling of

betalamic acid (**1**) and **2** in water to produce OxiBeet (**3**). The structures of betanin, the main

starting material of **1**, and pBeet are shown for comparison. (b) High-resolution mass spectrum

of OxiBeet; *m/z* 303.0976 [M]⁺; Calc'd.: 303.0975. (c) ¹H, ¹³C, and [¹H,¹³C] heteronuclear single

quantum coherence (HSQC) spectra of OxiBeet (70 µmol L⁻¹, 800 MHz/200 MHz, D₂O at 288

9

K). Atomic numbering is shown in red. Assignment of the signals in the NMR spectra was supported by quantum mechanical gauge-including atomic orbital (GIAO) calculations (Fig. S3).

To examine the behavior of OxiBeet in an aqueous solution, we compared the pH dependence of its observed first-order hydrolysis rate constant (k_{obs}) at 60 °C with those of pBeet and betanin (Figs. 2a and S4–S7). Under neutral and slightly alkaline conditions, OxiBeet was found to be far more stable than betanin. However, all the compounds were shown to be subject to acid-catalyzed decomposition (Fig. 2a). Deprotonation of the nitrone group (pK_a 4.4, Fig. S8) increases the negative charge density at N1 in the 1,7-diazaheptamethinium system (Fig. 2b) and shifts the absorption maximum of OxiBeet to shorter wavelengths (blue shift, ca. 2000 cm^{-1}, Fig. 2c). Such a shift is not observed for pBeet, which readily undergoes hydrolysis in alkaline conditions. Natural betalains are hydrolyzed under alkaline conditions, and the synthesis of a more stable analog was reported to require extensive modification of the betalain framework.[31]

The biocompatibility of OxiBeet was tested using the human hepatic cell line HepaRG, which is a well-established model for studying drug metabolism and toxicity because it retains many characteristics of primary human hepatocytes.[32] Cells incubated with the betalain nitrone (0.1 mmol L^{-1} to 1 µmol L^{-1}) for 6 h remained 100% viable, and 1 mmol L^{-1} OxiBeet was required to reduce cell viability by 8–10% (Fig. 2d).
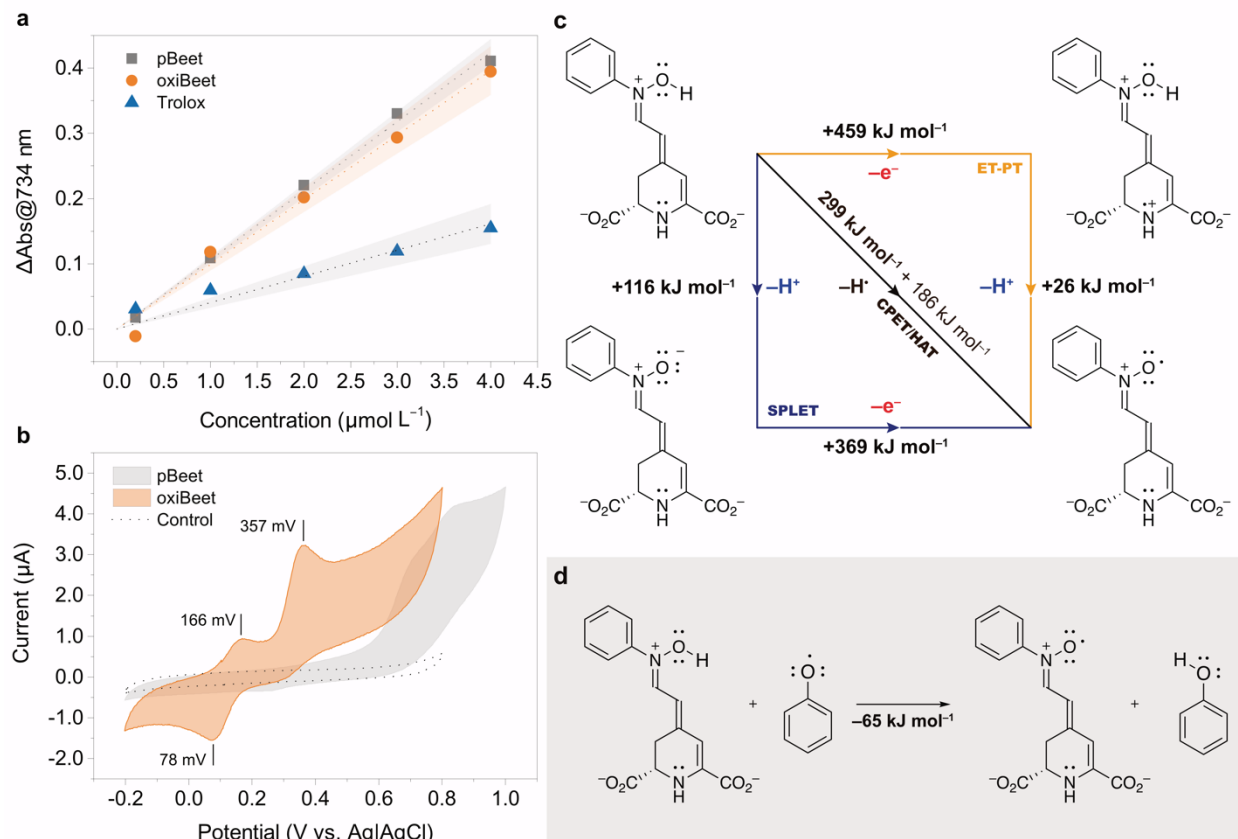
Figure 2. Properties of OxiBeet in aqueous solution. (a) Effect of pH on the logarithm of observed rate constants (k_{obs}, min^{-1}) for the decomposition of OxiBeet and pBeet at 60 °C; equivalent data for Betanin, reproduced from Ref. 33, is shown for comparison. (b) Partial charges of the nitrogen atoms of OxiBeet and its protonated (N–OH) form according to the Merz–Kollman–Singh (MKS) scheme. (c) Contour plots showing the absorbance spectra of OxiBeet and pBeet as a function of pH; red indicates UV–Vis absorbance values of ~0.5, and individual spectra for selected pH values are plotted above each contour plot. (d) Viability of HepaRG cells treated with OxiBeet (1 mmol L^{-1} to 1 μmol L^{-1}, 6 h) was measured by using the MTT assay. Negative control experiments were carried out using 1% FBS DMEM; cells incubated with Triton X-100 (1% v/v in PBS) were used as positive controls. Asterisks indicate

levels of statistical significance, as obtained via a one-way ANOVA with Geisser–Greenhouse correction and Dunnett's multiple comparison test ($N = 5$): (*) $P = 0.02$ and (***) $P = 0.0002$.

The ability of nitrones to react with oxidants has broad applicability.[1, 2] To assess the antioxidant potential of OxiBeet, we measured its radical scavenging capacity and redox potential. At pH 7.4, the radical scavenging capacities of OxiBeet and pBeet determined using the TEAC/ABTS[+•] method[23] are identical at the 95% confidence level (TEAC = 3.8 ± 0.1, Fig. 3a). However, the oxidation of the 1,7-diazaheptamethinium system of OxiBeet occurred at a much lower potential than those of other betalains,[14] including pBeet,[34] as evidenced by the intense irreversible anodic response at 357 mV vs. Ag|AgCl. Moreover, OxiBeet nitrone was reversibly oxidized to the corresponding nitroxide; anodic potential (E_{pa}) = 166 mV, cathodic potential (E_{pc}) = 78 mV, and half-wave potential ($E_{1/2}$) = 124 mV, Fig. 3b. Despite being non-phenolic, OxiBeet is a potent reducing agent and its TEAC is higher than those of well-known antioxidants such as gallic acid, vitamin C, vitamin E, and many flavonoids.[35, 36]

Enthalpies of electron (e[−]), proton (H^{+}) and hydrogen atom (H[•]) transfer were calculated using quantum chemical methods to determine the preferred thermodynamic pathway for the oxidation of OxiBeet.[37-39] The homolytic bond dissociation energy (BDE) of the NO–H bond of OxiBeet was found to be at least 70 kJ mol^{−1} lower than the energy required for the competing electron transfer in the sequential proton loss electron transfer (SPLET) or electron transfer followed by proton transfer (ET-PT) pathways, as shown in Fig. 3c. Therefore, the occurrence of concerted proton-coupled electron transfer (concerted PCET), that is, hydrogen atom transfer (HAT) or concerted proton-electron transfer (CPET), is favored over stepwise processes. In addition, the −65 kJ mol^{−1} change in enthalpy of the isodesmic reaction between the phenoxyl radical and

OxiBeet was much lower than the values reported for pBeet (–11 kJ mol^{-1})[34] and its phenolic analog (*p*-OH-pBeet, –32 kJ mol^{-1})[20]. These results are in agreement with the electrochemical and theoretical data and highlight the ease with which OxiBeet can be oxidized.

Figure 3. Antioxidant capacity and redox profile of OxiBeet. (a) Change in absorbance (ΔAbs) of ABTS$^{+\bullet}$ at 734 nm after 6 min of reaction as a function of antioxidant concentration for OxiBeet, pBeet, and Trolox in phosphate buffer (pH 7.4, 50 mmol L^{-1}). (b) Cyclic voltammograms of OxiBeet and pBeet in 0.1 mol L^{-1} KCl and negative control (dotted line, 0.1 mol L^{-1} KCl$_{(aq)}$); glassy carbon electrode, Ag|AgCl (KCl sat.), scan rate: 50 mV s^{-1}, [betalain] = 88 µmol L^{-1}. (c) More O'Ferrall–Jencks diagram for the ionization and 1e$^-$-oxidation of OxiBeet.
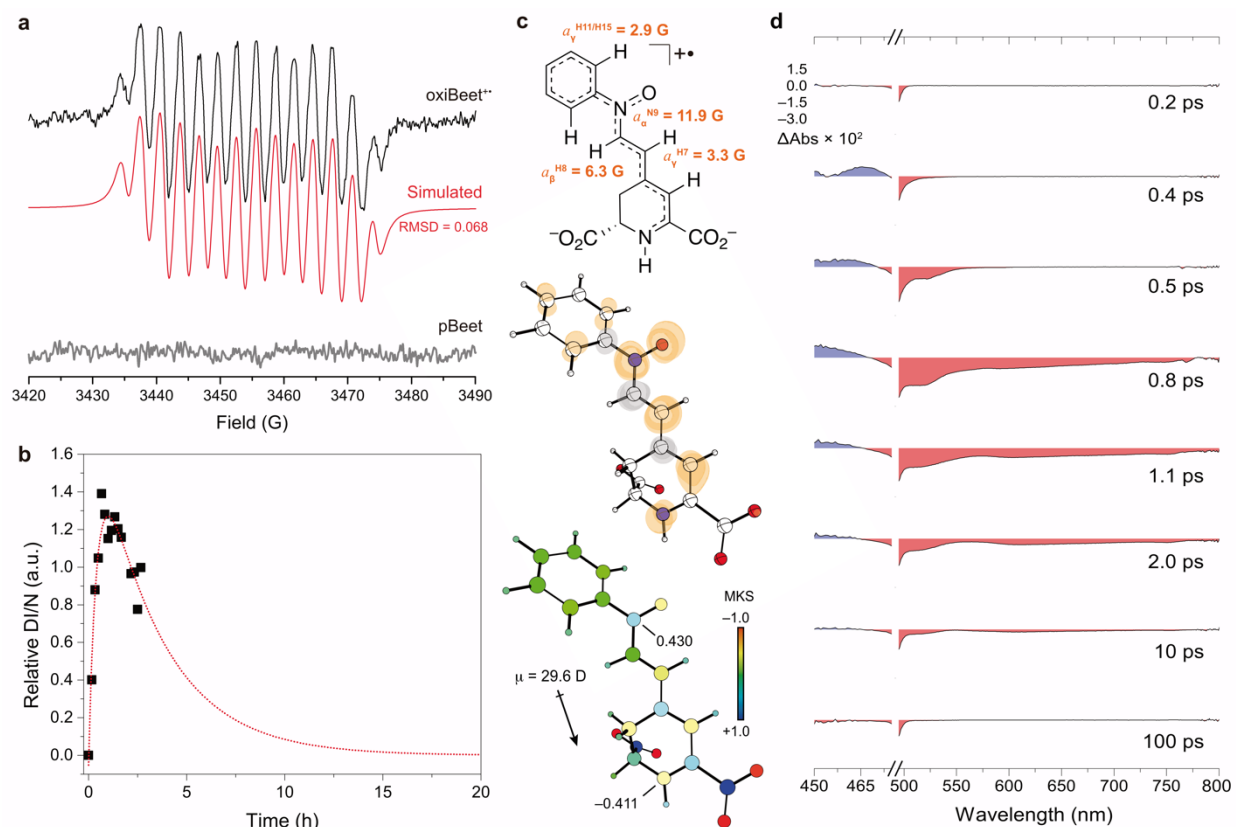
Compounds are presented as dicarboxylates as this is the expected major form in aqueous solution at pH > 4.[33] Energies refer to the enthalpy changes between states; a value of 186 kJ mol^{-1} in the concerted pathway is required for the 1e$^-$-oxidation of H$^\bullet$ to produce H$^+$ and e$^-$. (d) Isodesmic reaction between the phenoxyl radical and OxiBeet to produce phenol and OxiBeet$^{+\bullet}$.

A solution of OxiBeet in phosphate buffer at pH 7.4 was saturated with molecular oxygen for 1 min at room temperature to promote its autoxidation. The EPR spectrum of the product shows a 14-line pattern, indicating a delocalized NO radical with the following hyperfine coupling constants (hfcc, in Gauss): $a_\alpha^N = 11.9$, $a_\beta^H = 6.3$, $a_\gamma^H = 3.3$ and $a_\gamma^{2H} = 2.9$ (Fig. 4a). This result is compatible with the existence of a delocalized nitroxide 1,7-diazaheptamethinyl radical cation of OxiBeet, as determined by EPR simulation. An EPR response was not observed for control experiments using pBeet. The value of k_{obs} for the formation of OxiBeet$^{+\bullet}$ was $(6.5 \pm 1.4) \times 10^{-4}$ s^{-1} (half-life, $\tau_{1/2} = 18$ min, excess O$_2$, pseudo-first order conditions), while its decomposition rate constant was much lower ($k_{obs} = (8.8 \pm 2.7) \times 10^{-5}$ s^{-1}, lifetime, $\tau = 2.5$ h, $\tau_{1/2} = 106$ min) (Figs. 4b and S9). For comparison, $\tau_{1/2}$ values for the superoxide adducts of the widely used pyrroline N-oxide spin traps DMPO (5,5-dimethyl-1-pyrroline N-oxide), EMPO (5-(ethoxycarbonyl)-5-methyl-1-pyrroline N-oxide), and CDMPO (2-carboxy-5,5-dimethyl-1-pyrroline N-oxide) are 0.9, 9.9, and 27.5 min, respectively.[40]

The positive spin density of OxiBeet$^{+\bullet}$ was found to be localized on the N1, C5, C7, and N9 atoms (Fig. 4c), which provides additional support for our structure assignment. The partial positive charges at the N1 and N9 atoms increase upon 1e$^-$-oxidation of OxiBeet, as expected considering charge delocalization arguments. Although studies on the reaction between betanin and radicals have been performed using EPR spectroscopy,[41] this report demonstrates for the first

time that the 1,7-diazaheptamethinium scaffold increases the stability of nitroxide radicals. Thus, these findings highlight the contribution of the 1,7-diazaheptamethinium system of betalains to their striking antioxidant properties.[20, 34]

Ultrafast transient absorption experiments were carried out to determine whether photoexcitation plays a role in the autoxidation of OxiBeet. In aerated water, the electronic excitation of OxiBeet at 485 nm results in ground state bleaching (Fig. 4d). The acquired transient spectra revealed a positive absorption band at 450 nm, which was assigned to the excited state absorption ($S_1 \rightarrow S_n$; $n > 1$), and a negative band at about 520 nm that was attributed to S_0 depletion. The broad negative absorption band centered at approximately 625 nm was attributed to $S_1 \rightarrow S_0$ stimulated emission, which was observed after 800 fs and ceased to exist after 10 ps. In fact, similar results were obtained for betanin[42] as were produced for OxiBeet in the present study: full ground state recovery occurs less than 100 ps after photoexcitation, which precludes the possibility of the occurrence of an $S_1 \rightarrow T_1$ intersystem crossing, and photoproducts were not formed in noticeable amounts.

Figure 4. Electronic spin structure of OxiBeet$^{+\bullet}$ and photophysical data. (a) Observed (black) and simulated (red) hyperfine EPR spectra of OxiBeet$^{+\bullet}$ in phosphate buffer, pH 7.4, at 298 K. The lack of response for pBeet is shown for comparison. The color of the solution remained unchanged during the experiment. (b) Kinetics of formation and disappearance of OxiBeet$^{+\bullet}$; the dotted red line is a nonlinear fit of the data to a biexponential function. (c) Spin density distribution and partial charges of the nitrogen atoms of OxiBeet$^{+\bullet}$; red and blue indicate positive and negative spin densities, respectively. The hfcc values for OxiBeet$^{+\bullet}$ calculated by simulation are given in the overlaid orange text. (d) Transient absorption spectra of OxiBeet in water; pump wavelength: 485 nm.

CONCLUSIONS

The repertoire of multifunctional nitrones has been expanded by the design and synthesis of a prototypical betalain-nitrone based on the *N*-oxide 1,7-diazaheptamethinium scaffold. OxiBeet is based on a chiral starting material obtained from renewable sources and can be conveniently synthesized and purified in water. This pseudo-natural product is a potent antioxidant that was demonstrated to be non-cytotoxic in a HepaRG cell model, within a concentration range typically used in biological assays. Moreover, it is oxidized via concerted PCET and is stable towards hydrolysis under neutral and alkaline aqueous conditions, characteristics that give it a clear advantage over its betalain counterparts. The formation of the resonance-stabilized cation radical of OxiBeet upon autoxidation enables the development of antioxidants that can inhibit oxygen-induced changes in industrial products and demonstrates the importance of the 1,7-diazaheptamethinium system for the antioxidant properties of betalains in general. These findings indicate that OxiBeet and its analog betalain-nitrones can be potentially used as biocompatible antioxidants, redox mediators, and spin traps, opening new perspectives for the development of therapeutics for diseases associated with oxidative stress.

ASSOCIATED CONTENT

Supporting Information

The following supporting information is available free of charge.

Supplementary methods.

Cartesian coordinates of the optimized structures.

Figure S1. UV-Vis spectra of OxiBeet.

Figure S2. pH dependence of the molar absorption coefficient of OxiBeet.

Figure S3. Correlation between the experimental ^{1}H and ^{13}C chemical shifts obtained for OxiBeet and the isotropic shielding calculated by using the GIAO method.

Figure S4. Effect of pH on the absorption spectra of OxiBeet over time.

Figure S5. Effect of pH on the kinetics of decomposition of OxiBeet.

Figure S6. Effect of pH on the absorption spectra of pBeet over time.

Figure S7. Effect of pH on the kinetics of decomposition of pBeet.

Figure S8. Effect of pH on the emission spectra of OxiBeet and pBeet and corresponding titration curves and speciation plots.

Figure S9. Selected EPR spectra of OxiBeet solution at room temperature as a function of time.

AUTHOR INFORMATION

Corresponding Author

*elbastos@iq.usp.br

Author Contributions

E.L.B. conceived the study. E.L.B. and A.C.P wrote the paper. E.L.B., A.C.P., R.B.F., L.C.E., C.O.M., F.A.D., E.P., Y.H., J.S. and A.M.C.F. designed the experiments. A.C.P., R.B.F., L.C.E., C.O.M., F.A.D., and Y.H. performed the experimental work. E.L.B. carried out theoretical calculations. All authors discussed and interpreted the results.

REFERENCES

1.   Floyd, R. A.; Kopke, R. D.; Choi, C. H.; Foster, S. B.; Doblas, S.; Towner, R. A., Nitrones as therapeutics. *Free Radic. Biol. Med.* **2008,** *45* (10), 1361–1374.

2.   Oliveira, C.; Benfeito, S.; Fernandes, C.; Cagide, F.; Silva, T.; Borges, F., NO and HNO donors, nitrones, and nitroxides: Past, present, and future. *Med. Res. Rev.* **2018,** *38* (4), 1159–1187.

3.   Marco-Contelles, J., Recent advances on nitrones design for stroke treatment. *J. Med. Chem.* **2020,** *63* (22), 13413–13427.

4.   Murahashi, S. I.; Imada, Y., Synthesis and transformations of nitrones for organic synthesis. *Chem. Rev.* **2019,** *119* (7), 4684–4716.

5.   Bagryanskaya, E. G.; Krumkacheva, O. A.; Fedin, M. V.; Marque, S. R. A., Development and application of spin traps, spin probes, and spin labels. *Methods Enzymol.* **2015,** *563*, 365–396.

6.   Waldman, A. J.;   Ng, T. L.;   Wang, P.; Balskus, E. P., Heteroatom-heteroatom bond formation in natural product biosynthesis. *Chem. Rev.* **2017,** *117* (8), 5784–5863.

7.   Rosselin, M.;   Poeggeler, B.; Durand, G., Nitrone derivatives as therapeutics: From chemical modification to specific-targeting. *Curr. Top. Med. Chem.* **2017,** *17* (18), 2006–2022.

8.   Rodrigues, T.; Reker, D.; Schneider, P.; Schneider, G., Counting on natural products for drug design. *Nat. Chem.* **2016,** *8* (6), 531–541.

9.   Socrier, L.; Rosselin, M.; Gomez Giraldo, A. M.; Chantemargue, B.; Di Meo, F.; Trouillas, P.;   Durand, G.; Morandat, S., Nitrone-Trolox conjugate as an inhibitor of lipid oxidation: Towards synergistic antioxidant effects. *Biochim. Biophys. Acta, Biomembr.* **2019,** *1861* (8), 1489–1501.

10.   Quina, F. H.; Bastos, E. L., Chemistry inspired by the colors of fruits, flowers and wine. *An. Acad. Bras. Cienc.* **2018,** *90* (1 Suppl 1), 681–695.

11.   Prior, R. L.; Cao, G., Antioxidant phytochemicals in fruits and vegetables: diet and health implications. *HortScience* **2000,** *35* (4), 588–592.

12.   Kugler, F.; Stintzing, F. C.; Carle, R., Evaluation of the antioxidant capacity of betalainic fruits and vegetables. *J. Appl. Bot. Food Qual.* **2007,** *81* (1), 69–76.

13.   Kanner, J.;   Harel, S.; Granit, R., Betalains – A new class of dietary cationized antioxidants. *J. Agric. Food Chem.* **2001,** *49* (11), 5178–5185.

14.   Slimen, I. B.;   Najar, T.; Abderrabba, M., Chemical and antioxidant properties of betalains. *J. Agric. Food. Chem.* **2017,** *65* (4), 675–689.

15. Ciriminna, R.; Fidalgo, A.; Danzì, C.; Timpanaro, G.; Ilharco, L. M.; Pagliaro, M., Betanin: A bioeconomy insight into a valued betacyanin. *ACS Sust. Chem. Eng.* **2018,** *6* (3), 2860–2865.

16. Rahimi, P.; Abedimanesh, S.; Mesbah-Namin, S. A.; Ostadrahimi, A., Betalains, the nature-inspired pigments, in health and diseases. *Crit. Rev. Food Sci. Nutr.* **2019,** *59* (18), 2949–2978.

17. Hadipour, E.; Taleghani, A.; Tayarani-Najaran, N.; Tayarani-Najaran, Z., Biological effects of red beetroot and betalains: a review. *Phytother. Res.* **2020,** *34* (8), 1847–1867.

18. Apak, R.; Ozyurek, M.; Guclu, K.; Capanoglu, E., Antioxidant activity/capacity measurement. 1. Classification, physicochemical principles, mechanisms, and electron transfer (ET)-based assays. *J. Agric. Food. Chem.* **2016,** *64* (5), 997–1027.

19. Polturak, G.; Aharoni, A., "La vie en rose": Biosynthesis, sources, and applications of betalain pigments. *Mol. Plant.* **2018,** *11* (1), 7–22.

20. Gonçalves, L. C. P.; Lopes, N. B.; Augusto, F. A.; Pioli, R. M.; Machado, C. O.; Freitas-Dörr, B. C.; Suffredini, H. B.; Bastos, E. L., Phenolic betalain as antioxidants: *meta* means more. *Pure Appl. Chem.* **2020,** *92* (2), 243–253.

21. Pioli, R. M.; Mattioli, R. R.; Esteves, L. C.; Dochev, S.; Bastos, E. L., Comparison of the effect of *N*-methyl and *N*-aryl groups on the hydrolytic stability and electronic properties of betalain dyes. *Dyes Pigm.* **2020,** *183*, 108609.

22. Schliemann, W.; Kobayashi, N.; Strack, D., The decisive step in betaxanthin biosynthesis is a spontaneous reaction. *Plant. Physiol.* **1999,** *119* (4), 1217–1232.

23. Re, R.; Pellegrini, N.; Proteggente, A.; Pannala, A.; Yang, M.; Rice-Evans, C., Antioxidant activity applying an improved ABTS radical cation decolorization assay. *Free Radic. Biol. Med.* **1999,** *26* (9-10), 1231–1237.

24. Stoll, S.; Schweiger, A., EasySpin, a comprehensive software package for spectral simulation and analysis in EPR. *J. Magn. Reson.* **2006,** *178* (1), 42–55.

25. Polturak, G.; Aharoni, A., Advances and future directions in betalain metabolic engineering. *New Phytol.* **2019,** *224* (4), 1472–1478.

26. Rodrigues, A. C. B.; Mariz, I. D. A.; Macoas, E. M. S.; Tonelli, R. R.; Martinho, J. M. G.; Quina, F. H.; Bastos, E. L., Bioinspired water-soluble two-photon fluorophores. *Dyes Pigm.* **2018,** *150*, 105–111.

27. Doherty, S.; Knight, J. G.; Backhouse, T.; Summers, R. J.; Abood, E.; Simpson, W.; Paget, W.; Bourne, R. A.; Chamberlain, T. W.; Stones, R.; Lovelock, K. R. J.; Seymour, J. M.; Isaacs, M. A.; Hardacre, C.; Daly, H.; Rees, N. H., Highly selective and solvent-dependent reduction of nitrobenzene to n-phenylhydroxylamine, azoxybenzene, and aniline catalyzed by phosphino-modified polymer immobilized ionic liquid-stabilized AuNPs. *ACS Catal.* **2019,** *9* (6), 4777–4791.

28. Stintzing, F. C.; Kugler, F.; Carle, R.; Conrad, J., First C-13-NMR assignments of betaxanthins. *Helv. Chim. Acta* **2006,** *89* (5), 1008–1016.

29. Wybraniec, S.; Nowak-Wydra, B.; Mizrahi, Y., ^{1}H and ^{13}C NMR spectroscopic structural elucidation of new decarboxylated betacyanins. *Tetrahedron Lett.* **2006,** *47* (11), 1725–1728.

30.   Stintzing, F. C.; Conrad, J.; Klaiber, I.; Beifuss, U.; Carle, R., Structural investigations on betacyanin pigments by LC NMR and 2D NMR spectroscopy. *Phytochemistry* **2004,** *65* (4), 415–422.

31.   Freitas-Dörr, B. C.; Machado, C. O.; Pinheiro, A. C.; Fernandes, A. B.; Dörr, F. A.; Pinto, E.; Lopes-Ferreira, M.; Abdellah, M.; Sa, J.; Russo, L. C.; Forti, F. L.; Gonçalves, L. C. P.; Bastos, E. L., A metal-free blue chromophore derived from plant pigments. *Sci. Adv*. **2020,** *6* (15), eaaz0421.

32.   Donato, M. T.;   Jover, R.; Gomez-Lechon, M. J., Hepatic cell lines for drug hepatotoxicity testing: Limitations and strategies to upgrade their metabolic competence by gene engineering. *Curr. Drug Metab*. **2013,** *14* (9), 946–968.

33.   Esteves, L. C.; Pinheiro, A. C.; Pioli, R. M.; Penna, T. C.; Baader, W. J.; Correra, T. C.; Bastos, E. L., Revisiting the mechanism of hydrolysis of betanin. *Photochem. Photobiol.* **2018,** *94* (5), 853–864.

34.   Nakashima, K. K.; Bastos, E. L., Rationale on the high radical scavenging capacity of betalains. *Antioxidants* **2019,** *8* (7), 222.

35.   Foti, M. C.; Amorati, R., Non-phenolic radical-trapping antioxidants. *J. Pharm. Pharmacol*. **2009,** *61* (11), 1435–1448.

36.   Gulcin, I., Antioxidants and antioxidant methods: an updated overview. *Arch. Toxicol*. **2020,** *94* (3), 651–715.

37.   Darcy, J. W.; Koronkiewicz, B.; Parada, G. A.; Mayer, J. M., A continuum of proton-coupled electron transfer reactivity. *Acc. Chem. Res*. **2018,** *51* (10), 2391–2399.

38. Warren, J. J.; Tronic, T. A.; Mayer, J. M., Thermochemistry of proton-coupled electron transfer reagents and its implications. *Chem. Rev.* **2010,** *110* (12), 6961–7001.

39. Weinberg, D. R.; Gagliardi, C. J.; Hull, J. F.; Murphy, C. F.; Kent, C. A.; Westlake, B. C.; Paul, A.; Ess, D. H.; McCafferty, D. G.; Meyer, T. J., Proton-coupled electron transfer. *Chem. Rev.* **2012,** *112* (7), 4016–4093.

40. Ouari, O.; Hardy, M.; Karoui, H.; Tordo, P., Recent developments and applications of the coupled EPR/Spin trapping technique (EPR/ST). In *Electron Paramagnetic Resonance*, Gilbert, B. C.; Murphy, D. M.; Chechik, V., Eds. Royal Society of Chemistry: Cambridge, 2010; Vol. 22, pp 1–40.

41. Esatbeyoglu, T.; Wagner, A. E.; Motafakkerazad, R.; Nakajima, Y.; Matsugo, S.; Rimbach, G., Free radical scavenging and antioxidant activity of betanin: electron spin resonance spectroscopy studies and studies in cultured cells. *Food Chem. Toxicol.* **2014,** *73*, 119–126.

42. Wendel, M.; Nizinski, S.; Tuwalska, D.; Starzak, K.; Szot, D.; Prukala, D.; Sikorski, M.; Wybraniec, S.; Burdzinski, G., Time-resolved spectroscopy of the singlet excited state of betanin in aqueous and alcoholic solutions. *Phys. Chem. Chem. Phys.* **2015,** *17* (27), 18152–18158.

SYNOPSIS

The preparation and characterization of OxiBeet, a biocompatible, antioxidant betalain-nitrone that has broad biomedical applicability, is presented.

TOC/Abstract graphic

Novel bio-based antioxidant nitrone scaffold

Betalains from beetroots: Renewable feedstock

Semisynthesis + purification **IN WATER**

• Inexpensive • Biocompatible
• Antioxidant • Water-soluble
• Radical precursor • EPR-ready